

Acoustic Edge Modes of the Degenerate Two-Dimensional Electron Gas Studied by Time-Resolved Magnetotransport Measurements

G. Ernst, R. J. Haug,* J. Kuhl, K. von Klitzing, and K. Eberl

Max-Planck-Institut für Festkörperforschung, Heisenbergstrasse 1, 70569 Stuttgart, Germany

(Received 27 June 1996)

Edge magnetoplasmons propagating along the smooth boundary of a two-dimensional electron gas are studied by time-resolved magnetotransport experiments. The incident pulse splits up into several pulses due to modal dispersion. The observed delay times are well described by the predictions of Aleiner and Glazman for the fundamental and acoustic modes [Phys. Rev. Lett. **72**, 2935 (1994)], if the quantized Hall conductance is taken into account. [S0031-9007(96)01655-9]

PACS numbers: 73.20.Mf, 73.40.Hm, 73.50.Jt

Plasma oscillations of a two-dimensional electron gas (2DEG) acquire remarkable properties in the presence of a perpendicular magnetic field [1]. While the excitation of bulk plasmons requires a frequency equal to or larger than the cyclotron frequency ω_c , the spectrum of edge excitations remains gapless. The direction of allowed k vectors for these low energy excitations is determined by the confining potential and the direction of the Lorentz force acting on the moving carriers. For a given k vector, the edge magnetoplasmon (EMP) frequency decreases with increasing magnetic field.

Experimentally, EMPs were discovered as low frequency eigenmodes of a confined 2DEG realized in a semiconductor heterostructure [2] or on the surface of liquid helium [3,4]. The EMP propagation direction was detected by phase sensitive measurements of the induced voltage on small electrodes around the perimeter of the 2DEG [5]. Time-domain measurements demonstrated the unidirectionality of the EMP motion in the quantum Hall effect (QHE) and the fractional QHE regime in a more intuitive way [6]. Using a 2DEG with a screening metallic electrode close by, the propagation of EMP wave packets confined to quantum Hall edge channels was identified in time-domain measurements [7].

Recently, additional edge modes were observed, which were characterized by a resonance frequency below the frequency of the conventional EMP mode. An indication of a novel EMP mode was found in the nondegenerate 2DEG on the surface of liquid helium [8], which was explained in terms of oscillations of the boundary. A different set of EMP modes, for which the resonance frequency increased with increasing magnetic field, was observed for positive ions in a circular geometry [9]. These modes were identified with the edge modes predicted by Nazin and Shikin for a circular sheet of electrons on liquid helium with a smooth boundary [10].

The theoretical description of plasma oscillations in a 2DEG starts with a seemingly simple set of elementary electrodynamic equations [1,11], which have to be solved self-consistently, in order to obtain the EMP dispersion relation. Since the electric fields are not restricted to the

plane of the 2DEG, the problem is truly three dimensional. Analytic solutions could be obtained in a number of limiting cases (for a review, see [1]), and it was realized early that a smooth electron density profile permits additional (so called acoustic) EMP modes [1,10]. For a 2DEG in a semiconductor heterostructure, the dispersion relation for the fundamental mode $\omega_0(k)$ and the acoustic modes $\omega_j(k)$ (with $j > 0$) was calculated recently by Aleiner and Glazman [12]:

$$\begin{aligned}\omega_0(k) &= [n_s e / (2\pi \epsilon_0 \epsilon_r B)] k \ln(e^{-\gamma} / 2ka) & j = 0 \\ \omega_j(k) &= [n_s e / (2\pi \epsilon_0 \epsilon_r B)] k / j & j = 1, 2, \dots\end{aligned}\quad (1)$$

(n_s is the bulk 2D electron density, $\epsilon_0 \epsilon_r$ the effective dielectric constant of the surrounding medium, γ the Euler constant, and $a \sim 10a_B$ the width of the boundary strip, where the EMP charge is localized, with a_B being the Bohr radius in GaAs.)

In the fundamental ω_0 mode, the charge density oscillates only in the direction parallel to the boundary. The acoustic ω_j modes are characterized by j additional nodes in the electron density variation appearing in the perpendicular direction. In [12], the decay rates were calculated in addition, and observability conditions for the fundamental and acoustic modes were established. The decay rates were found to be mode dependent, and increase with increasing mode index j . Furthermore, the decay rates are k vector dependent, and large k vectors are necessary for the acoustic modes to avoid overdamping.

Here, we report on the observation of acoustic modes in time-domain measurements. The 2DEG was contained in a GaAs/AlGaAs heterostructure, i.e., the system for which the EMP dispersion and damping were calculated in [12]. Applying short electrical pulses to our samples, we are able to excite EMPs with sufficiently large k vectors. Thus, a clear identification of the signals belonging to the fundamental and acoustic EMP modes is possible. We observe that both the propagation velocity and the damping of the transmitted pulses are affected by the QHE. Therefore a modification of the existing theory [12] is necessary for a complete description of our data.

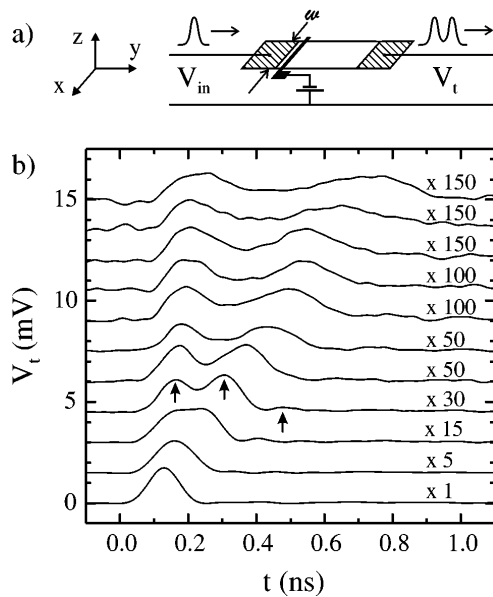


FIG. 1. (a) Sketch of the sample geometry and measurement setup. (b) Evolution of the signal transmitted through the 2DEG with increasing magnetic field between 0 T (bottom curve) and 2 T, in intervals of 0.2 T. All data are taken at 1.5 K, the incident pulse having an amplitude of 10 mV and a width of 100 ps. Curves for different magnetic fields are offset by $150 \mu\text{V}$ each. A splitting of the incident pulse into three transmitted pulses (marked by arrows in the transmitted signal measured at 0.6 T) appears due to modal dispersion.

Figure 1(a) schematically shows the measurement setup. A strip geometry is etched into a high-mobility GaAs/ $\text{Al}_x\text{Ga}_{1-x}\text{As}$ heterostructure. Ohmic contacts in the form of microstriplines with an impedance of 50Ω are attached at both ends. A $10 \mu\text{m}$ wide top gate crosses the 2DEG close to one of the contacts. The bottom side of the sample is metalized and serves as ground. The 2DEG has a carrier concentration of $n_s = 2.0 \times 10^{15} \text{ m}^{-2}$, a low-temperature mobility of $\mu = 80 \text{ m}^2/\text{Vs}$, and is located 148 nm below the surface. Two samples differing only in their sizes have been used: sample A, with a length of $320 \mu\text{m}$ and a width of $80 \mu\text{m}$, and sample B, which is 1.5 mm long and $390 \mu\text{m}$ wide. A short voltage pulse with an amplitude of 10 mV and a width of about 100 ps is applied to one of the contacts. The transmitted signal is measured with a time resolution of 80 ps using a broadband preamplifier and a fast sampling oscilloscope. The top gate serves to eliminate direct cross talk between input and output. First, a measurement is taken with the top gate grounded, then a reference measurement is recorded with a bias set to deplete the 2DEG underneath the gate. By subtracting these two time traces, we obtain the signal transmitted through the 2DEG itself [13]. Additionally, the sample input is terminated by a 50Ω resistance to avoid reflections caused by impedance mismatch. The measured traces demonstrate that the remaining reflections are in fact negligible. Details of the pulse generation and detection are given in [14]. All measurements were performed in a ^4He -cryostat at $T = 1.5 \text{ K}$.

In Fig. 1(b), the signals transmitted through sample A are shown for magnetic fields between 0 and 2 T, at 1.5 K, the amplitude of the input pulse being $V_{\text{in}} = 10 \text{ mV}$. In the presence of a small magnetic field, the transmitted pulse is affected only by the two-terminal resistance of the sample: The shape of the input pulse is maintained, and the decrease in amplitude is a consequence of the high-frequency current being distributed between the increasing two-terminal resistance of the sample and the 50Ω termination. With increasing magnetic field, an additional broadening of the transmitted peak is observed, and finally the peak splits into two separate peaks. Both peaks are comparable in amplitude. As the magnetic field is further increased, the positions of both peaks shift to later times, and their amplitudes continue to decrease. By looking more carefully at the data, a third peak can be identified, which displays a similar magnetic field dependence. The positions of these peaks are defined by fitting a Gaussian wave form to each of them. They are marked by arrows in the transmitted signal measured at 0.6 T.

In the presence of a magnetic field, the applied voltage pulse generates EMPs at the injection contact, which propagate along the edge of the sample until they reach the detection contact. Classical electrodynamics requires that certain boundary conditions at the injection contact must be fulfilled at all times. Therefore, the frequencies of the excited EMPs are determined by the Fourier components of the input pulse, and the k vectors are defined by the EMP dispersion relation. Figure 2 shows the dispersion

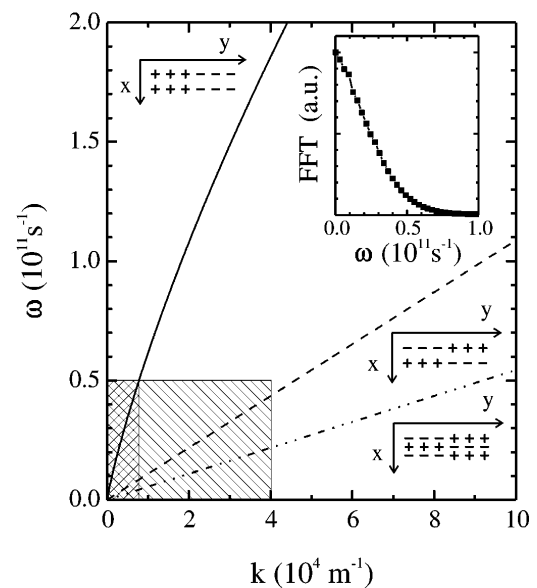


FIG. 2. Dispersion of the fundamental (solid line), and first (dashed line) and second (dash-dotted line) acoustic EMP mode at $B = 1 \text{ T}$, calculated using Eq. (1) with $n_s = 2.0 \times 10^{15} \text{ m}^{-2}$ and $\epsilon_r = 5.3$. The charge distributions in the different EMP modes are sketched near the corresponding dispersions. The inset depicts the Fourier transform of the input pulse from the measurements of sample A. The hatched area shows the range of accessible (k, ω) values for sample A, and the cross-hatched area for the wider sample B.

relations for the three lowest EMP modes at $B = 1$ T, together with a sketch of the charge density distributions in these modes. Comparing the frequencies in the incident pulse (see inset of Fig. 2) with the EMP frequencies, it can be seen that applying pulses in the time domain gives access to large k vectors. However, the width of the injection contact defines an upper boundary for the accessible k vectors. The resulting ranges in the (k, ω) plane for the two samples are marked in Fig. 2. Although our frequencies are in the range up to about $0.5 \times 10^{11} \text{ s}^{-1}$ (see inset of Fig. 2) and therefore large in comparison with typical measurements in the frequency domain [1,5], they are still small compared to the cyclotron energy. Hence, we cannot excite bulk magnetoplasmons or high-frequency EMPs, which both have frequencies larger than ω_c [1,11,15].

The splitting of the incident pulse into several transmitted pulses originates from modal dispersion in the 2DEG. The incident pulse excites EMPs of the fundamental mode and of the first and second acoustic modes. With increasing magnetic field, the group velocities $v_g = \partial\omega_j/\partial k$ decrease, the transmitted signals arrive with larger delays, and modal dispersion becomes observable. For the quantitative analysis, we obtain the parameters (amplitude, delay, and width) of the transmitted pulses by fitting Gaussian wave forms to the measured signals. The transmission delay t_d is then defined with respect to the measured delay at $B = 0$ T. Figure 3(a) shows the transmission delays of

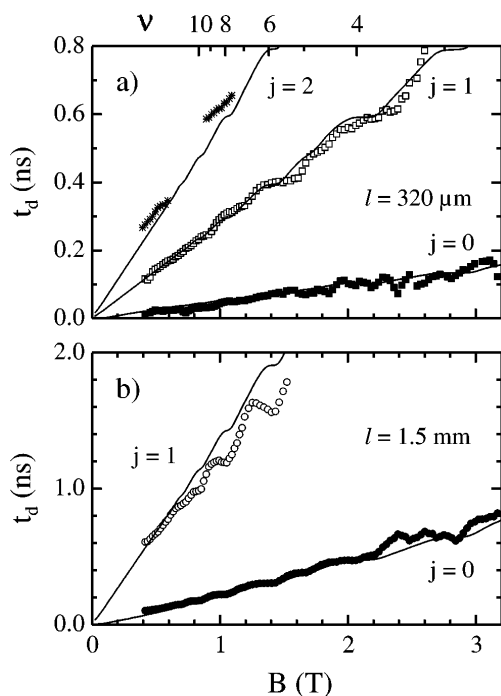


FIG. 3. (a) Dependence of the transmission delay t_d of the first (full squares), second (open squares), and third (stars) transmitted pulses on the applied magnetic field for sample A. Solid lines show the delay times of the $j = 0, 1, 2$ modes according to the modified Eq. (1) (see text). (b) t_d of the first (full circles) and second (open circles) peaks for sample B together with the theoretical prediction (solid lines).

the three pulses for sample A. In agreement with Eq. (1), the transmission delays increase with increasing magnetic field. Additionally, plateaus around integer filling factors appear. We include the observed plateaus in Eq. (1) by replacing the classical $n_s e/B$ by the quantized σ_{xy} measured on a reference sample from the same wafer. This modification is in accordance with earlier calculations and measurements of the fundamental EMP mode [1,6], and reflects the importance of bulk currents which are necessary for the charging of the edge region for the fundamental mode as well as for the acoustic modes. The comparison between theory and experiment is then straightforward. The dispersion relation for the first acoustic mode [Eq. (1) with $j = 1$] is used to determine the only adjustable parameter, the effective dielectric constant ϵ_r of the surrounding material. From this fit, we obtain $\epsilon_r = 5.3$. For the case of a half space filled with GaAs, one expects $\epsilon_r = (\epsilon_{\text{GaAs}} + 1)/2 \approx 7$. In our experiment, however, we confined the 2DEG by etching away the surrounding heterostructure. Therefore, the EMP electric field extends into a space that is less than half-filled with GaAs, which results in a smaller value for ϵ_r .

The dispersion relation for the fundamental mode contains an additional logarithmic factor involving the k vector. In order to compare our experimental data with Eq. (1), we decompose the input pulse into partial waves, inject them as EMPs, let them propagate, and superpose the transmitted EMPs at the detection contact. The calculated delays in both samples arising from the fundamental mode and the first and second acoustic modes are shown in Fig. 3 as solid lines, using the same value of $\epsilon_r = 5.3$ for all modes. The agreement with the experimental data is astonishingly good. The comparison between samples A and B gives additional evidence for the correctness of our interpretation. For sample B, only the $j = 0, 1$ EMP modes could be identified, and the observed transmission delays indeed scale with the length of the sample. The delay times for the fundamental mode are also in reasonable agreement with those obtained in [6], where the pulse propagation along the 1.7 mm long circumference of a circular 2DEG was studied. In these experiments, acoustic EMPs might have been excited as well. However, the circular sample geometry (without absorbing Ohmic contacts) did not allow their identification, because the acoustic EMP pulses will arrive at the detection gate after several round trips of the fundamental EMP pulse and be obscured by signals from the fundamental EMP pulse. Furthermore, the amplitude of the acoustic modes suffers from stronger damping with respect to the fundamental mode, which adds to the difficulties in their observation during subsequent round trips of the fundamental mode.

Interestingly, the observed plateaus in the transmission delays are wider than expected from resistance measurements at the same temperature, and the plateau values also deviate slightly. Both deviations show that replacing the classical σ_{xy} by the quantized Hall conductance is not sufficient in order to account for the differences between a

classical (nondegenerate) 2DEG and the highly degenerate 2DEG in a heterostructure sample. Of course, the actual electron density profile in our sample might differ from the one assumed in Eq. (1), in which case the numerical prefactors change slightly (compare, e.g., results obtained in [15–17]). This uncertainty appearing already in the classical description might account for the deviations in the plateau values, but not for the larger plateau widths. Therefore, the observed deviation could be a hint towards the influence of the magnetic field dependent electronic structure at the edge [18] on these time-resolved transport experiments.

The relative amplitude of the observed modes is a measure of the relative oscillator strength averaged over the frequencies in the input pulse. In [12] the oscillator strength for the different modes has been calculated assuming incident plane waves. It was found that the oscillator strength decreases with increasing mode index, and that the logarithmic factor $|\ln(|ka|)|$ determines the relative values. Thus, large k vectors are favorable for the observation of acoustic modes. Since the incident electric field in our experiment is not a pure plane wave, the results obtained in [12] need to be modified for a quantitative description. However, the oscillator strength in our experimental setup will decrease drastically for k vectors larger than π divided by the width of the injection contact w , which leads to $k_{\max} = 4 \times 10^4 \text{ m}^{-1}$ for sample A and $k_{\max} = 0.8 \times 10^4 \text{ m}^{-1}$ for sample B. In Fig. 2, the situation is depicted for $B = 1 \text{ T}$. For sample A, we find that the $j = 2$ mode and all higher modes suffer from the k vector restriction, while for sample B, already the $j = 1$ mode is subject to a reduced range of frequencies that couple to this mode. And indeed, we find experimentally that the $j = 2$ mode has a much smaller amplitude compared to the $j = 0, 1$ modes for sample A, and that for sample B, the oscillator strength of the $j = 1$ mode is already significantly smaller than for the $j = 0$ mode.

Although the dispersion relations for the fundamental and acoustic modes in the modified Eq. (1) account very well for the observed transmission delays, some small but systematic deviations arise between our measurements and the formulas given in [12] concerning the damping of these modes. According to [12], the characteristic length of the charge spreading $l_\omega = e^2 n_s / 4\pi \epsilon_r \epsilon_0 m \omega \omega_c^2 \tau$ has to be smaller than the characteristic length scale $a/(j+1)$ for the charge distribution in the j th mode. Assuming the width of the charged strip at the boundary to be $a \sim 10a_B$ [12], and using the average frequency $\bar{\omega} = 3 \times 10^{10} \text{ s}^{-1}$ in our input signals and the measured transport scattering time $\tau_{\text{tr}} = 30 \text{ ps}$, we expect to observe acoustic EMP modes only for magnetic fields $B > 2 \text{ T}$. In Fig. 1(b), however, pulse splitting due to modal dispersion appears already at smaller magnetic fields $B \approx 0.6 \text{ T}$. Furthermore, the damping calculated in [12] is significantly larger than observed in our experiments. We attribute these deviations to the differences between a classical 2DEG for which the theory in [12] is valid and the degenerate 2DEG

in our samples. It is well known that the boundary region in the QHE regime is divided into alternating strips of compressible and incompressible electron liquids [18]. While the corresponding changes in the electron density profile are expected to affect the dispersion relations significantly for modes $j > \sqrt{a/a_B}$, the damping rate should be reduced in all modes, as the dissipation is suppressed within the incompressible regions [12].

In conclusion, we have presented time-resolved magnetotransport experiments in a 2DEG, where we observed a splitting of the incident pulse due to modal dispersion. From the magnetic field dependence of the propagation delays, we identified the observed modes as the fundamental, and first and second acoustic EMP modes, for which the dispersion relations were recently calculated [12].

We thank S. Mikhailov, V. Falko, and N. Zhitenev for useful discussions and D. Heitmann and D. Galpin for critical reading of the manuscript.

*Present address: Institut für Festkörperphysik, Appelstrasse 2, D-30167 Hannover, Germany.

- [1] V. A. Volkov and S. A. Mikhailov, Zh. Eksp. Teor. Fiz. **94**, 217 (1988) [Sov. Phys. JETP **67**, 1639 (1988)].
- [2] S. J. Allen, Jr., H. L. Störmer, and J. C. M. Hwang, Phys. Rev. B **28**, 4875 (1983).
- [3] D. B. Mast, A. J. Dahm, and A. L. Fetter, Phys. Rev. Lett. **54**, 1706 (1985).
- [4] D. C. Glattli, E. Y. Andrei, G. Deville, J. Poitrenaud, and F. I. B. Williams, Phys. Rev. Lett. **54**, 1710 (1985).
- [5] P. J. M. Peters, M. J. Lea, A. M. L. Jansen, A. O. Stone, W. P. N. M. Jacobs, P. Fozzoni, and R. W. van der Heijden, Phys. Rev. Lett. **67**, 2199 (1991).
- [6] R. C. Ashoori, H. L. Stormer, L. N. Pfeiffer, K. W. Baldwin, and K. West, Phys. Rev. B **45**, 3894 (1992).
- [7] N. B. Zhitenev, R. J. Haug, K. v. Klitzing, and K. Eberl, Phys. Rev. Lett. **71**, 2292 (1993).
- [8] O. I. Kirichek, P. K. H. Sommerfeld, Y. P. Monarkha, P. J. M. Peters, Y. Y. Kovdya, P. P. Steijaert, R. W. van der Heijden, and A. T. A. M. Waele, Phys. Rev. Lett. **74**, 1190 (1995).
- [9] P. L. Elliott, C. I. Pakes, L. Skrbek, and W. F. Vinen, Phys. Rev. Lett. **75**, 3713 (1995).
- [10] S. S. Nazin and V. B. Shikin, Zh. Eksp. Teor. Fiz. **94**, 133 (1988) [Sov. Phys. JETP **67**, 288 (1988)].
- [11] A. L. Fetter, Phys. Rev. B **32**, 7676 (1985).
- [12] I. L. Aleiner and L. I. Glazman, Phys. Rev. Lett. **72**, 2935 (1994).
- [13] For the range of frequencies present in our input pulses, this procedure is sufficient to suppress the capacitive part of the transmitted signal.
- [14] G. Ernst, R. J. Haug, M. Klingenstein, J. Kuhl, K. v. Klitzing, and K. Eberl, Appl. Phys. Lett. **68**, 3752 (1996).
- [15] X. Xia and J. J. Quinn, Phys. Rev. B **50**, 11 187 (1994).
- [16] I. L. Aleiner, D. Yue, and L. I. Glazman, Phys. Rev. B **51**, 13 467 (1995).
- [17] S. A. Mikhailov, Pis'ma Zh. Eksp. Teor. Fiz. **61**, 412 (1995) [JETP Lett. **61**, 418 (1995)].
- [18] D. B. Chklovskii, B. I. Shklovskii, and L. I. Glazman, Phys. Rev. B **46**, 4026 (1992).